Environmental Science & Technology

Article

pubs.acs.org/est

Efficient Isoprene Secondary Organic Aerosol Formation from a Non-IEPOX Pathway

Jiumeng Liu,[†,◆] Emma L. D'Ambro,[‡,◆] Ben H. Lee,[§] Felipe D. Lopez-Hilfiker,[§] Rahul A. Zaveri,[†] Jean C. Rivera-Rios,[∥] Frank N. Keutsch,[∥] Siddharth Iyer,[⊥] Theo Kurten,[⊥] Zhenfa Zhang,[#] Avram Gold,[#] Jason D. Surratt,[#] John E. Shilling,*[,†,▽] and Joel A. Thornton*[,‡,§,○]

[†]Atmospheric Sciences and Global Change Division, Pacific Northwest National Laboratory Richland, Washington 99352, United States

[‡]Department of Chemistry and [§]Department of Atmospheric Sciences, University of Washington, Seattle, Washington 98195, United States

[∥]Paulson School of Engineering and Applied Sciences and Department of Chemistry and Chemical Biology, Harvard University, Cambridge, Massachusetts 02138, United States

[⊥]Department of Chemistry, University of Helsinki, Helsinki FI-00014, Finland

[#]Department of Environmental Sciences and Engineering, University of North Carolina, Chapel Hill, North Carolina 27599, United States

Supporting Information

ABSTRACT: With a large global emission rate and high reactivity, isoprene has a profound effect upon atmospheric chemistry and composition. The atmospheric pathways by which isoprene converts to secondary organic aerosol (SOA) and how anthropogenic pollutants such as nitrogen oxides and sulfur affect this process are subjects of intense research because particles affect Earth's climate and local air quality. In the absence of both nitrogen oxides and reactive aqueous seed particles, we measure SOA mass yields from isoprene photochemical oxidation of up to 15%, which are factors of 2 or more higher than those typically used in coupled chemistry climate models. SOA yield is initially constant with the addition of increasing amounts of nitric oxide (NO) but then sharply decreases for input concentrations above 50 ppbv. Online measurements of aerosol molecular composition show that the fate of second-generation RO_2 radicals is key to understanding the efficient SOA formation and the NO_x-dependent yields described here and in the literature. These insights allow for improved quantitative estimates of SOA formation in the preindustrial atmosphere and in biogenic-rich regions with limited anthropogenic impacts and suggest that a more-complex representation of NO_x-dependent SOA yields may be important in models.

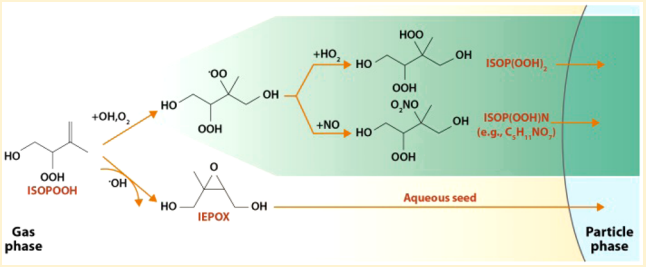

INTRODUCTION

Global forests emit 500 to 750 Tg of isoprene per year, the largest flux of biogenic or anthropogenic nonmethane hydrocarbons to the atmosphere.[1] Isoprene-derived secondary organic aerosol (iSOA) is predicted to comprise a significant fraction of the organic aerosol (OA) burden over large regions of the globe.[2−5] Isoprene also influences the oxidative capacity of the troposphere, particularly in pristine forested regions,[6,7] due to its high reactivity toward atmospheric radicals and its effect on the fate of reactive nitrogen oxides, with consequences for the abundance and lifetime of greenhouse gases such as methane and tropospheric ozone, and likely indirect effects on particle formation, growth,[8] and SOA yield from other VOCs.[9] There is thus great interest in resolving the atmospheric fate of isoprene-derived carbon.

Recently, there has been significant interest in determining whether anthropogenic pollutants,[8,10] such as NO_x and sulfur oxides, may enhance iSOA formation and thereby increase the climate effects of aerosol particles, which directly interact with solar radiation and alter the reflectivity and life cycle of clouds. The magnitude of this anthropogenic forcing of a natural aerosol formation process has been difficult to quantify with certainty,[11] in part because the iSOA formation potential under preindustrial "pristine" conditions is poorly known. The net anthropogenic aerosol forcing of climate is determined by referring to year 1750 conditions, when NO_x and sulfur emissions were approximately 4 and 6 times lower, respectively, than they are today.[12] Thus, assessing the anthropogenic aerosol forcing is inherently tied to accurately quantifying natural aerosol sources under preindustrial conditions.[10] This need, in turn, requires a mechanistic-level understanding of the iSOA formation pathways.

Received: April 15, 2016
Revised: August 6, 2016
Accepted: August 22, 2016
Published: August 22, 2016

DOI: 10.1021/acs.est.6b01872
Environ. Sci. Technol. 2016, 50, 9872−9880

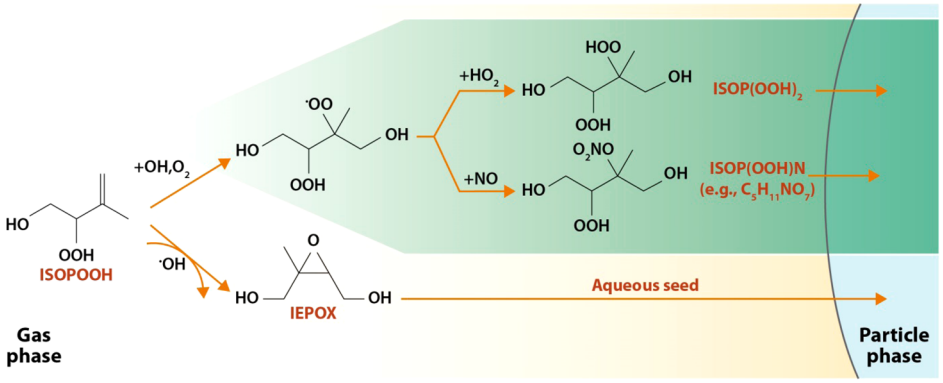

Figure 1. Simplified reaction mechanism of ISOPOOH, a first-generation isoprene photooxidation product, with the described ISOP(OOH)$_2$ pathway based on our observations included. SOA formation from IEPOX chemistry (bottom pathway)[12,15] was not observed in these experiments (see Figure S7).

In the atmosphere, isoprene reacts with hydroxyl radicals (OH) to form reactive organic peroxy radical intermediates (ISOPO$_2$). The short-lived (~100 s in forests)[13] ISOPO$_2$ intermediates ultimately react with hydroperoxyl radicals (HO$_2$), nitric oxide (NO), or other organic peroxy radicals (RO$_2$). The HO$_2$ pathway, estimated to account globally for one-half of the reactive fate of ISOPO$_2$[11] and possibly more in the preindustrial atmosphere, produces a hydroxy hydroperoxide (ISOPOOH); see Figure 1. In remote regions and in the preindustrial atmosphere, where both NO and HO$_x$ concentrations are low, the ISOPO$_2$ radical also isomerizes to produce hydroperoxyaldehyde species.[11,14]

Most recent experiments have focused on iSOA formed from the multiphase acid-catalyzed chemistry of ISOPOOH-derived epoxydiols (IEPOX).[12,15−19] However, measurements of iSOA yield under low-NO$_x$ conditions in the absence of reactive aqueous seed particles should be revisited, particularly in light of recent findings of significant wall artifacts.[20] These conditions likely represent much of the preindustrial atmosphere and remote pristine regions in the present day, where isoprene is oxidized far from anthropogenic emissions. Moreover, most previous experiments studying photochemical iSOA formation were conducted under conditions in which the oxidant field and, thus, product branching is continuously changing and where the important iSOA-forming products are apparently lost to the walls of the reaction chamber and, thus, undetected.[20] In addition, most models that do include a NO$_x$ dependence of SOA yields classify them as either high-NO$_x$ or NO$_x$-free, while studies have suggested that NO$_x$ dependence for iSOA is more complex.[5,21,22] Addition of NO$_x$ has been shown to change the relative branching ratios of isoprene RO$_2$ radicals reacting with HO$_2$ and NO, but the dynamic NO$_x$ dependence of iSOA yield is not mechanistically well-understood and therefore difficult to accurately parametrize for inclusion in models. These issues suggest a continued need for additional studies of iSOA formation.

Here, we report results from a series of laboratory studies in which we systematically investigate photochemical iSOA formation as a function of the branching between isoprene-derived peroxy radical reactions with hydroperoxyl (HO$_2$) and nitric oxide (NO) radicals. Our experiments were operated in the continuous-flow mode, which provides an alternative approach to most previous studies. We measure iSOA yields that are significantly higher than most literature values and that are dependent on both H$_2$O$_2$ and NO concentrations. We also show that this approach can have lower wall-loss effects (due to equilibration) and simplifies the kinetic interpretation of the experimental results by investigating steady-state periods. That is, iSOA yields are obtained for a predetermined extent of aging, set by oxidant concentrations and chamber residence time, as opposed to batch-mode experiments in which products are continuously passing through several photochemical generations, which might have significantly different iSOA production and loss terms. We use a box model based on a detailed chemical mechanism to investigate the oxidant fields and thus infer production pathways of online-measured gas- and condensed-phase compounds. Our results demonstrate a pathway for efficient iSOA formation independent of IEPOX chemistry and may be important in regions of the atmosphere far removed from anthropogenic influence.

EXPERIMENTAL SECTION

Chamber Experiment Overview. Experiments were conducted in the Pacific Northwest National Laboratory (PNNL) 10.6 m^3 Teflon environmental chamber.[23] The chamber was flushed with purified air from AADCO pure air generators until the particle concentration was less than 1 particle cm^{-3} before the start of continuous-mode experiments. Isoprene, and/or NO in purified air were injected from calibrated gas cylinders with flows regulated by MKS mass flow controllers. H$_2$O$_2$ was introduced into the chamber by passing pure air through a gently heated glass bulb, with the H$_2$O$_2$ solution (Sigma-Aldrich, 50 wt % in H$_2$O) continuously injected into the bulb using a syringe pump. Relative humidity was controlled at 50%, by passing pure air at a variable flow rate through pure water (18.2 MΩ cm, < 5ppbv TOC). (NH$_4$)$_2$SO$_4$ seed particles were first produced by an atomizer, passed through a diffusion dryer, then size-selected to a mobility diameter of 50 nm using a DMA, and injected into the chamber; number concentrations of seed particles ranged between 1800 and 3000 cm^{-3}. UV black lights (Q-Lab, UVA-340) were turned on to initiate photooxidation. We continuously monitored the UV intensity with a radiometer and measured a stable UV flux equivalent to an NO$_2$ photolysis rate of J_{NO_2} = 0.16 min^{-1}, which corresponds to a H$_2$O$_2$ photolysis rate of approximately 2.8 × 10^{-3} min^{-1}. Total flow rate through the chamber was 34 Lpm, resulting in a 5.2 h chamber residence time. For each experiment, steady-state periods were at least 18 h after the start of each experiment. The injections of isoprene, H$_2$O$_2$, UV lights, or a combination of these

DOI: 10.1021/acs.est.6b01872
Environ. Sci. Technol. 2016, 50, 9872−9880

Table 1. Table of Isoprene Photooxidation Experimental Conditions and Results[a]

experiment no.	input [isoprene] (ppbv)	input [H_2O_2] (ppmv)	input [NO] (ppbv)	chamber [isoprene] at steady state (ppbv)	Δ [isoprene] (ppbv)	[HO_2][b] (ppbv)	$f_{RO_2HO_2}$[c] (%)	aerosol mass[d] ($\mu g/m^3$)	yield[d] (%)
				low-NO_x conditions					
1	183	5	0	41.1	141.9	0.19	99.3	19.5	4.8
2	76	15	0	13.4	62.2	0.53	99.8	22.1	12.5
3	26	15	0	4.6	21.7	0.55	99.9	9.1	14.7
4	26	5	0	4.7	21.7	0.30	99.9	4.6	7.5
5	26	10	0	4.5	21.8	0.44	99.9	6.7	10.8
6	26	15	0	4.4	22.0	0.55	99.9	7.7	12.4
7	26	10	0	4.4	22.0	0.44	99.9	5.1	8.2
				high-NO_x conditions					
8	26	10	2	4.0	22.4	0.44	96.9	6.6	10. 5
9	26	10	5	3.6	22.7	0.44	93.6	6.2	9.6
10	26	10	10	3.2	23.1	0.44	89.7	7.6	11.6
11	26	10	20	3.4	22.9	0.44	84.1	6.5	10.0
12	26	10	50	1.9	24.4	0.43	74.1	1.9	2.7

[a]Input concentrations refer to the concentrations of the reactants that would be in the chamber if there were no loss mechanisms, including any chemistry. [b][HO_2] was determined using the UWCM model. [c]The fraction of second-generation RO_2 reacting with HO_2, calculated from eq 1, assuming k_{isom} = 0.002 s^{-1} based on Crounse et al. (2011).[11] [d]Both SOA aerosol mass concentration and SOA yield are corrected for particle wall losses. Corrections for gas-phase wall loss are not applied as they are not significant in these experiments.

were periodically halted to perform blank experiments. A summary of experimental conditions is listed in Table 1.

Instruments. A suite of online instruments was used to characterize both the gas- and particle-phase composition. The evolution of isoprene concentrations throughout each experiment were determined by an Ionicon quadrupole proton-transfer-reaction mass spectrometry (High-Sensitivity PTR-QMS 500, Ionicon Analytik, Austria).[24] Many isoprene photooxidation products, of both the gas and the particle phases, were monitored by the University of Washington high-resolution time-of-flight chemical-ion-mass-spectrometry coupled with a filter-inlet for gases and aerosols (FIGAERO HR-ToF-CIMS).[25,26] Particle-phase mass and chemical composition were measured with an Aerodyne high-resolution time-of-flight mass spectrometer (HR-ToF-AMS).[27,28] Number and volume concentrations of the aerosols formed in the chamber were measured with a TSI scanning mobility particle sizer (SMPS Model 3081). An NO−NO_2−NO_x analyzer (Thermo Environmental models 42c and 42i) was used to measure concentration of NO and NO_x. The detection limit of the instrument is 0.4 ppbv (1 min averaging time) and, for most conditions, the steady-state NO concentration with the lights on (i.e., during experiments) was below the instrument detection limit. Therefore, steady-state NO concentrations were calculated using a photochemical model described below. We note that input NO concentrations were well-defined as NO was delivered from a calibrated gas cylinder using mass flow controllers and concentrations were verified during periods when lights were turned off. A UV absorption O_3 analyzer (Thermo Environmental Instruments model 49C) allowed for the measurement of O_3 concentration. Detailed descriptions of HR-ToF-CIMS and HR-ToF-AMS can be found in the Supporting Information as well as in previous publications.[25,26,28−30]

ISOPOOH Experiment. In addition to forming SOA from isoprene photooxidation, a series of experiments was conducted using an authentic isoprene 4-hydroxy-3-hydroperoxy (4,3-ISOPOOH) standard, one of the two main atmospherically important ISOPOOH isomers.[31] The 4,3-ISOPOOH was dissolved in water, placed in a glass bulb, and gently warmed pure air was passed through the bulb to carry ISOPOOH into the chamber. Reaction conditions were similar to those used in the isoprene oxidation experiments; RH was 50%, and 50 nm solid ammonium sulfate seed (~2400 cm^{-3}) was present. ISOPOOH concentrations were monitored with the FIGAERO HR-ToF-CIMS. Condensed-phase products were detected by both the FIGAERO HR-ToF-CIMS and HR-ToF-AMS.

IEPOX Experiment. Several literature reports have shown that IEPOX uptake onto reactive aqueous seed particles can produce SOA in substantial yield.[15,19] To confirm that heterogeneous uptake of IEPOX to seed particles was not driving SOA formation in the present isoprene and ISOPOOH photooxidation experiments, we performed an experiment using an authentic IEPOX standard. Synthesized *trans*-β-IEPOX dissolved in ethyl acetate was placed in a glass bulb, and pure air was passed through the bulb and into the chamber. Conditions in the chamber were again identical to those in the isoprene experiments. IEPOX concentrations were monitored with the FIGAERO HR-ToF-CIMS and with PTR-MS (as a fragment at m/z 69). Condensed-phase products were detected by both the FIGAERO HR-ToF-CIMS and HR-ToF-AMS.

University of Washington Chemical Mechanism Model. The University of Washington Chemical Mechanism (UWCM) box model was used to model the chamber system. Note that the model was run to guide interpretation of the observed chemistry and SOA yields, but the SOA yield values we report do not depend on model calculations in any way. The mechanism and its previous applications are described in detail elsewhere.[32] Briefly, the UWCM incorporates the University of Leeds Master Chemical Mechanism v3.2[33] with customized updates to address new understanding regarding glycolaldehyde,[34] methyl glyoxal,[35] methyl vinyl ketone, and methacrolein reactions[36] and isoprene RO_2 isomerization,[37] as well as updates to ISOPOOH chemistry presented here. These include formation of dihydroxy dihydroperoxides ($ISOP(OOH)_2$) from ISOPOOH-derived peroxy radicals as well as their associated loss processes, including hydrogen abstraction and photolysis of hydroperoxide groups. The branching between ISOPOOH-derived peroxy radicals and IEPOX formation, the bimolecular reaction rate constants of the ISOPOOH-derived peroxy radicals, unimolecular isomerization rates, are technically

DOI: 10.1021/acs.est.6b01872
Environ. Sci. Technol. 2016, 50, 9872−9880

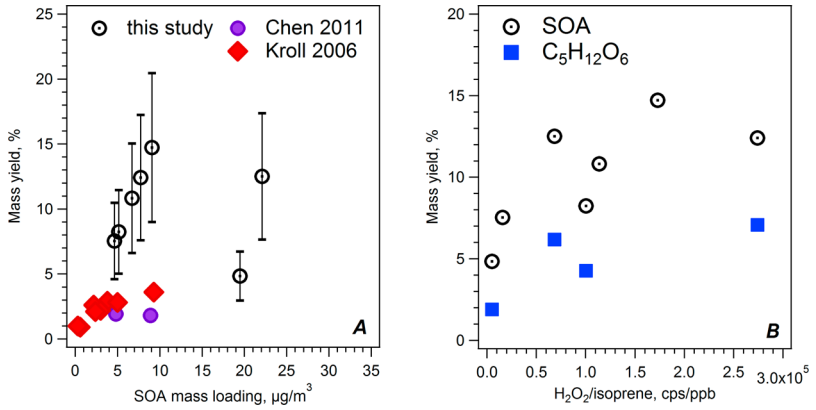

Figure 2. (A) iSOA yield as a function of mass loading for this and previous isoprene photooxidation experiments,[38,46] with error bars indicating uncertainties related to measurements and particle-phase wall loss correction; (B) dependence on the H_2O_2-to-isoprene ratio shown for the mass yield of SOA and $C_5H_{12}O_6$.

unknown. We use typical values of bimolecular rate constants for general RO_2 radicals found in the MCM and tune the branching ratio and isomerization rates to achieve agreement with the measured concentrations of ISOP(OOH)$_2$. The model was set up to incorporate conditions in the chamber such as the relative humidity, resonance time, photolysis frequencies, and temperature. Photolysis frequencies of H_2O_2 were tuned to match isoprene decays, and NO_2 photolysis frequencies were set to match measured values. Inputs specified for each experiment were the NO, isoprene, and H_2O_2 injection rates into the chamber.

RESULTS AND DISCUSSION

iSOA Formation under Low-NO_x Conditions. Figure 2 shows the results of the photochemical oxidation of 26−183 ppbv (input concentration) of isoprene in the absence of added NO (Table 1). Yields of iSOA were calculated based on measured steady-state organic aerosol mass loading and the amount of isoprene reacted, with only a particle wall loss correction applied (see the Supporting Information). We observed steady-state yield values up to 15% at a loading of 9 $\mu g\ m^{-3}$. Our yield values are generally higher for most conditions compared to those reported previously. In the presence of solid aerosol seeds, the iSOA mass yield has been reported to be <10% and usually <6%.[15,19,38−40] Higher transient yields, up to ∼9%, were observed in some batch mode experiments, but particle mass decreased as the experiment progressed, and the final yield values (e.g., yield after most isoprene has reacted) are more widely reported and incorporated into models.[38] We observed a dependence of the iSOA yield on the relative amounts of isoprene and H_2O_2 being continuously injected into the system, with higher H_2O_2-to-isoprene ratios generating higher iSOA yields (Figure 2B) under otherwise identical conditions.

The FIGAERO HR-ToF-CIMS measurements showed that compounds with a highly oxygenated and saturated carbon composition, such as $C_5H_{12}O_6$, contributed to ∼30−50% of the iSOA on average (Figure 2B). We identify the dominant $C_5H_{12}O_6$ compound as isoprene dihydroxydihydroperoxides (ISOP(OOH)$_2$ for short). Though these specific species have not been previously identified in iSOA particles,[6] previous studies have detected a high content of unresolved peroxides in OA under low-NO_x conditions,[38,41] ranging from 25% and 60% by mass in seeded and unseeded experiments, respectively. More recently, several studies have reported the detection of $C_5H_{12}O_6$ as an isoprene oxidation product in both the gas and the particle phases, but an accurate estimation of SOA mass yield from isoprene were lacking in those experiments.[42−44] In our experiments, the yield of particle-phase $C_5H_{12}O_6$ and related components scaled with H_2O_2 concentration, and therefore HO_2 concentration, in a similar manner to the overall iSOA yield (see Figure 2B), consistent with a later-generation product.

In the currently accepted isoprene oxidation mechanism, the reaction of ISOPOOH with OH forms IEPOX, with molar yield exceeding 75%.[6,45] IEPOX formation is in direct competition with the addition of molecular oxygen to the nascent carbon radical, which can also form a peroxy radical already containing both hydroxy and hydroperoxide functional groups. From the measured iSOA mass yield and the speciation of aerosol components, we infer that of order 10% of OH additions by number to the remaining carbon−carbon double bond in ISOPOOH result in the formation of the multifunctional organic peroxy radical, which, under the HO_2-dominant conditions of our experiment, go on to form a dihydroxydihydroperoxide, ISOP(OOH)$_2$, and related products, as shown in Figure 1. When this pathway is dominant, the iSOA mass yield can readily approach 15% due to the larger molar mass of ISOP(OOH)$_2$ relative to isoprene and to the additional Raoult's Law partitioning or reactive uptake of other semivolatile products to the particle phase without requiring the presence of reactive seed particles. Although we measured ISOP(OOH)$_2$ to be the most abundant single component in the particle phase, a myriad of other compositions were also detected under low NO_x conditions, including $C_5H_{12}O_5$ and $C_5H_{10}O_5$ (see Figure 3), suggesting that partitioning and reaction of other products are also important contributors to iSOA. Although our conclusions are not dependent upon mass closure, applying estimates of the HR-ToF-CIMS instrument detection efficiency to these and other compositions results in the sum of all detected species agreeing with the AMS measured total organic aerosol mass to well within the ±50% uncertainty of the FIGAERO HR-ToF-CIMS calibration (Figure 4B). This suggests the HR-ToF-CIMS captured a significant fraction of the total iSOA mass.

Starting with ISOPOOH instead of isoprene as the precursor, Krechmer et al. (2015) and Riva et al. (2016) observed some of the same products in the gas phase and the particle phase, respectively, and proposed the same reaction pathway.[42,43] Although the Riva study did not provide an estimate of the mass yield of iSOA, the Krechmer study estimated an iSOA yield of 4.2% by applying significant corrections to their measurements

DOI: 10.1021/acs.est.6b01872
Environ. Sci. Technol. 2016, 50, 9872−9880

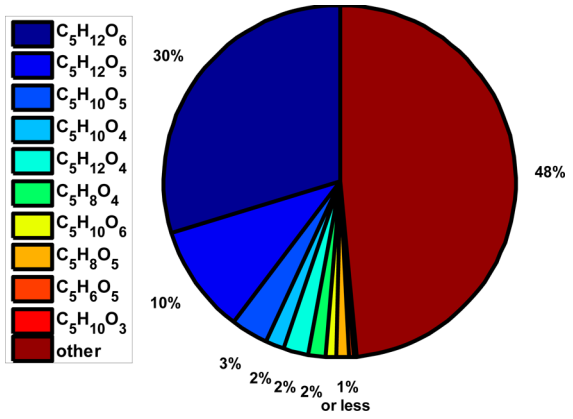

Figure 3. Mass fractions of the total in the particle-phase detected by the FIGAERO HR-ToF-CIMS in the low-NO_x experiments. The "other" group is composed of numerous compounds that make up, at most, a few percent of the total mass.

to account for gas-phase wall losses. The Krechmer et al. yield agrees reasonably with our observations, considering that their reported uncertainty is a factor of 2.5[43] and the fact that semivolatile partitioning and multiphase organic reactions are likely more important to iSOA yields when isoprene is used as the precursor (our experiment) rather than ISOPOOH (Krechmer experiments), given the broader array of products present. We also performed ISOPOOH photooxidation experiments, and these same later-generation components are observed in the particle phase, but our observations showed the major condensed-phase compound is $C_5H_{12}O_6$ rather than the $C_5H_{10}O_5$ and $C_5H_{12}O_5$ implied by the Krechmer study (Figure S5). The differences are likely due to the relatively constant oxidation field in our continuous-mode experiments, our use of higher HO_2 levels than Krechmer et al., and the direct detection of aerosol molecular composition as opposed to that estimated from gas-phase abundance. The differences in oxidation field, reactant concentration, and aging time likely also explain the higher iSOA yield in these experiments compared to literature values (i.e., the Kroll study[38] and the Chen study[46]), as displayed in Figure 2. In addition, we directly observed significant differences in the condensed-phase product distribution when comparing our own isoprene and ISOPOOH experiments (Figures 3 and S5, respectively), which again suggests differences between the yield values for our isoprene experiments and the Krechmer ISOPOOH experiments could be caused by the use of different precursors. On the basis of our direct measurements of the aerosol composition, we therefore propose that the iSOA yield in the absence of both NO and aqueous seed particles is triggered in large part by the ISOPOOH-derived multifunctional organic peroxy radical chemistry.

Role of NO_x in iSOA Formation. As noted at the outset, a key question is whether anthropogenic emissions enhance iSOA formation efficiency. We probed this question and also gained insights into the proposed $ISOP(OOH)_2$ formation pathway by systematically increasing the NO concentration in the chamber while holding all other conditions constant. To our knowledge, we resolve, for the first time, the detailed molecular changes in iSOA composition as a function of NO_x using online methods. These experiments lead to a reduction in measured $ISOP(OOH)_2$ and iSOA yields and the production of organic nitrates (Figures S6), such as $C_5H_{11}O_7N$, which was detected also in ambient aerosol.[47] The dependence of the iSOA yield and $ISOP(OOH)_2$ and related components on the input NO-to-isoprene ratio is shown in Figure 4. As NO increased, the abundance of $ISOP(OOH)_2$ decreased monotonically, while a series of organic nitrates increased in both the gas and the particle phases. Interestingly, the iSOA yield was nearly constant at low NO until a threshold NO level was reached (input NO-to-VOC ratio of ~0.38). With further increases in NO concentrations, the iSOA yield decreased from ~12% to ~3%, accompanied by a decrease in the more highly oxygenated organic nitrates. Both the saturated composition of the $C_5H_{11}O_7N$ organic nitrate, i.e., H + N = 2(C + 1), and its nonmonotonic dependence on NO concentrations are consistent with the source being the second generation peroxy radical formed from ISOPOOH discussed above, supporting the overall importance of the non-IEPOX peroxy radical pathway.

Using the UWCM model, the above behaviors can be interpreted in terms of the fraction of RO_2 reacting with HO_2 and NO, which were calculated as follows:

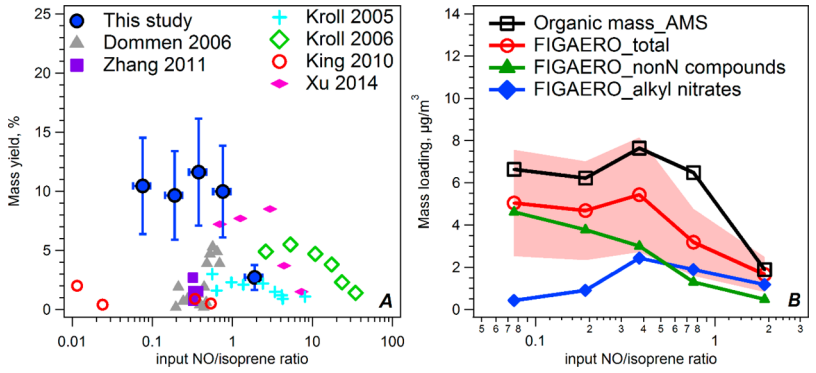

Figure 4. NO-to-isoprene ratio dependence of (A) SOA yield estimated from AMS, with results from previous studies as references,[22,38,40,48,53,54] and (B) approximate concentrations of the sum of non-N-containing C_5 compounds (green) and of alkyl nitrate compounds (blue) determined from FIGAERO HR-ToF-CIMS, plotted with the sum of both quantities and the AMS-measured total OA mass concentration. The error bars in (A) include uncertainty from both measurements and particle-phase wall loss corrections, and the shaded area in (B) indicates the ±50% uncertainty in FIGAERO HR-ToF-CIMS mass determination.

DOI: 10.1021/acs.est.6b01872
Environ. Sci. Technol. 2016, 50, 9872−9880

$$f_{RO_2HO_2} = \frac{HO_2 \cdot k_{RO_2HO_2}}{HO_2 \cdot k_{RO_2HO_2} + NO \cdot k_{RO_2NO} + RO_2 \cdot k_{RO_2RO_2} + k_{isom}} \quad (1)$$

$$f_{RO_2NO} = \frac{NO \cdot k_{RO_2NO}}{HO_2 \cdot k_{RO_2HO_2} + NO \cdot k_{RO_2NO} + RO_2 \cdot k_{RO_2RO_2} + k_{isom}} \quad (2)$$

where k_{RO_2NO}, $k_{RO_2HO_2}$, and $k_{RO_2RO_2}$ are the generic RO_2 rate constants obtained from the MCM,[33] and k_{isom} is the unimolecular RO_2 isomerization rate,[11] which is unknown for the ISOPOOH-derived organic peroxy radicals. Although k_{isom} may be important for setting the absolute values of $f_{RO_2HO_2}$ and f_{RO_2NO}, the relative behavior of the systematic addition of NO is independent of k_{isom}. Shown in Figure S8, the decrease in $ISOP(OOH)_2$ and iSOA is correlated with a decrease in the model predicted fraction of RO_2 reacting with HO_2, which reaches a value of ~0.75 at the highest steady-state mixing ratio of NO achieved in the chamber (~0.5 ppbv). The nonlinear effect of NO_x we observed can be explained by NO suppressing ISOPOOH formation, which is the source of the $C_5H_{11}O_6$ peroxy radical while, also enhancing the formation rate of highly oxygenated nitrates (Figure 4).

The combined effect of suppressed $ISOP(OOH)_2$ formation and the lower branching of RO_2 + NO to form multifunctional organic nitrates suggest that, all else being similar, anthropogenic increases in NO_x emissions have suppressed iSOA formation from the $ISOP(OOH)_2$ pathway in the present day atmosphere. Correlated changes in NO_x and OH abundance, which might have offsetting effects on iSOA concentrations (but not necessarily yields) require a more detailed chemical transport model treatment, which is beyond the scope of this paper. A nonlinear dependence of iSOA upon NO_x was observed in previous chamber studies,[21,38,48] but the chemistry is likely different in some cases because employing HONO as an OH and NO source strongly suppresses ISOPOOH chemistry and thus also the formation of the second-generation organic nitrates observed here.[22] RO_2 cross-reactions can be important depending upon the amount of isoprene reacting, but for the majority of these experiments, it was calculated by the UWCM to be a smaller fraction than reaction with HO_2 and NO (≪1%).

Our estimates of the production of the dihydroxy hydroperoxyl peroxy radical ($C_5H_{11}O_6$) from ISOPOOH + OH are derived from this model in comparison with the measured gas + aerosol abundance of the associated products (e.g., $C_5H_{12}O_6$, $C_5H_{12}O_5$, $C_5H_{11}O_7N$, and so on); see, e.g., Figure S8. Requiring 10% of ISOPOOH + OH to produce the $C_5H_{11}O_6$ peroxy radical (summed over all isomers) in the model adequately simulated the observed abundance and behavior of total (gas + particle) concentrations of $C_5H_{12}O_6$, presumed to be $ISOP(OOH)_2$. This version of the model does not simulate gas-particle partitioning or vapor wall loss of oxidation products. Oxidation products that would partition to the particle phase and possibly be protected from further oxidation reactions are therefore underestimated by the model. In addition, these data do not provide robust constraints on the isomerization rate of the proposed $C_5H_{11}O_6$ radicals; as such, there remains appreciable theoretical uncertainties associated with these calculations as well as those from measurement calibration. Nonetheless, the positive identification and measurement of a significant lower-limit fraction of iSOA mass being consistent with $ISOP(OOH)_2$ suggests the clear importance of this chemical pathway.

Contribution of IEPOX SOA to Observed iSOA Yield. Acid-catalyzed multiphase chemistry, especially of the isoprene epoxydiols (IEPOX), has been shown to be an important component of isoprene chemistry in the atmosphere.[6,15,49] Surratt et al. reported 30% iSOA mass yields in the presence of aqueous acidic seed particles (data not shown in Figure 2).[15] By using solid ammonium sulfate seed particles in our isoprene photooxidation experiments, we greatly suppressed the importance IEPOX chemistry. To confirm that these pathways were suppressed, we injected synthetic *trans*-β-IEPOX (>99% purity), which is the predominant isomer,[45] into the chamber in the presence of a high concentration of solid ammonium sulfate seed particles. No iSOA formation was detected (see Figure S7) despite the large concentrations of IEPOX (~15 ppbv) and seed particle surface area (~4.5×10^7 nm^2/cm^3). These results are consistent with literature reports showing that IEPOX requires reactive aqueous seed particles to generate SOA, while the seed particles were solid in our experiments. The iSOA in our photochemical experiments was thus formed with a high efficiency but from a mechanism that does not require acidity or aqueous inorganic ions.

Vapor Wall Loss in Continuous-Flow Chambers. Previous studies have shown that SOA yield measurements are often significantly biased low due to losses of semivolatile compounds to chamber walls.[20,50,51] Zhang et al. (2014) showed that aerosol mass yield in toluene photooxidation experiments increases with seed surface area in batch-mode experiments and suggested that a factor of 1.1−4.2 should be applied to chamber-measured SOA yields.[20] Constrained by α-pinene ozonolysis products observed in a short residence time (45 min) continuously stirred chamber, Ehn et al. (2014) also reported an increase in SOA corresponding to higher particle surface area.[51] Shilling et al. postulated that vapor-wall losses were lower in continuous-flow experiments relative to batch-mode experiments but did not conduct experiments that explicitly addressed this issue.[52]

To address gas-phase wall loss uncertainties, we systematically increased the injected ammonium sulfate seed surface area with other chamber conditions constant and representative of experiments described above (Δisoprene = 20 ppbv, 10 ppmv H_2O_2, 50% RH). This strategy has been previously described in the literature and is meant to increase the condensational sink rate to the aerosol phase to overcome condensational loss to the chamber walls.[20,51] We first added a second complete seed injection system identical to the first, which has the effect of doubling the monodisperse seed surface area while holding other factors, such as the size distribution, constant. As shown in Figure 5, we observed no increase in yield. We then further increased the seed surface area by decreasing the DMA sheath flow from 10 to 3 LPM, which decreased the DMA resolution (broadening the seed size distribution considerably) but increased the throughput. Finally, we bypassed the DMA and injected dry, polydisperse seed particles to further increase the seed surface area. Quantification of SOA deposited on the quasi-monodisperse and polydisperse seed is uncertain due to an increase in particle bounce from the AMS vaporizer and a decrease in particle transmission through the AMS lens; however, we saw no evidence for gas-phase wall loss (Figure 5). Details on collection efficiency corrections are given in the Supporting Information. If

DOI: 10.1021/acs.est.6b01872
Environ. Sci. Technol. 2016, 50, 9872−9880

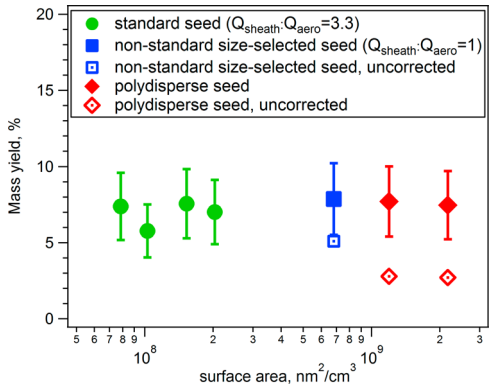

Figure 5. SOA yield as a function of particle surface area, with error bars indicating the measurement uncertainty. In experiments with broader seed-size distribution, SOA yields are corrected for the nonunity AMS collection efficiency by comparing aerosol volume concentrations determined from AMS and SMPS (see the Supporting Information). In all experiments, reaction conditions were controlled at 50% RH with a continuous injection of 20 ppbv isoprene and 10 ppmv H_2O_2.

partitioning to the chamber walls were a significant sink of SOA-forming species, we would expect to see SOA particle yield increase with increasing seed surface area,[20] which is clearly not the case for our data. Therefore, we conclude that net vapor-phase wall losses are minimal under our experimental conditions, and therefore, corrections for gas-phase wall loss are unnecessary. Such corrections would in theory only increase our iSOA yields, which are generally larger than most previous measurements without a correction. We hypothesize that the continued exposure of the chamber walls to semivolatile reaction products in continuous-mode experiments allows the gas phase to equilibrate with both the suspended particles and the walls, such that the net loss of gases to the walls is minimized for this chemical system. Fully understanding wall−gas interactions in continuous-flow chambers, the difference between continuous-flow chambers and batch chambers, and wall losses for other chemical systems requires further research.

In summary, we conducted continuous-flow chamber experiments and measured significant SOA yields of up to 15% from isoprene photooxidation under HO_2-dominated conditions and in the absence of heterogeneous IEPOX chemistry. Using a combination of gas- and particle-phase measurements, we identified a dihydroxy dihydroperoxide $ISO(POOH)_2$ and other multifunctional hydroperoxides as key condensing species and presented a chemical mechanism explaining their formation. We note that these experiments were designed to probe chemistry under HO_2-dominant conditions; therefore, HO_2 concentrations in the chamber are approximately 5−10 times higher than those typically found in the ambient atmosphere.[7,14] Lower HO_2 concentrations and longer aging times would likely reduce yield from this mechanism in the ambient atmosphere, and thus, iSOA yields presented herein should be regarded as upper limits. We investigated the effect of NO concentrations on this mechanism and found a complex relationship between SOA yield and NO_x. SOA yield was approximately constant with the addition of NO until a threshold was reached, after which additional NO dramatically reduced SOA yield. Gas- and particle-phase measurements showed that second-generation reaction products were again key to SOA formation, with decreasing yields explained by lower production of both second-generation multifunctional organic nitrates and second-generation multifunctional peroxides. Finally, we increased seed particle surface area while holding other reaction conditions constant and found no appreciable impact on SOA yield, implying that the net loss of gas-phase species to the chamber walls is minimized under these conditions.

Our results therefore point to a reaction pathway leading to the efficient formation of iSOA in the absence of NO_x and reactive seed particles, of which $ISOP(OOH)_2$ and its related peroxy radicals could be regarded as molecular tracers. This pathway, although a minor branch in competition with IEPOX formation, is a significant pathway in iSOA formation due to the production of low-volatility multifunctional hydroperoxide products. Accounting for shifts in the production and loss mechanisms of the second-generation isoprene photooxidation products, which have a strong sensitivity to ambient NO concentrations, will be important for determining iSOA in the preindustrial era or in remote regions with limited anthropogenic impacts with consequences for the calculation of a robust estimate of an anthropogenic forcing of aerosol−climate effects. Their abundance and particle-phase reactivity should thus be the focus of future laboratory and field experiments to better constrain their atmospheric fate and response to anthropogenic forcing.

■ ASSOCIATED CONTENT

Supporting Information

The Supporting Information is available free of charge on the ACS Publications website at DOI: 10.1021/acs.est.6b01872.

Detailed description of mass spectrometers used in this study, their operation, calibration and sensitivity (Table S1), and the particle-wall loss correction. Additional MS figures supporting analysis of organic aerosol (Figures S1−S6), the null results of an IEPOX uptake experiment (Figure S7), and modeled RO_2 branching ratios (Figure S8) are provided. (PDF)

■ AUTHOR INFORMATION

Corresponding Authors

*Phone: 206-543-4010; e-mail: thornton@atmos.uw.edu.
*Phone: 509-375-6874; e-mail: john.shilling@pnnl.gov.

Present Addresses

▽J.E.S.: Atmospheric Sciences and Global Change Division, Pacific Northwest National Laboratory Richland, WA 99352, United States.
○J.A.T.: Department of Chemistry, University of Washington, Seattle, WA 98195, United States.

Author Contributions

◆J.L. and E.L.D contributed equally to this manuscript.

Notes

The authors declare no competing financial interest.

■ ACKNOWLEDGMENTS

This research is based on work supported by the U.S. Department of Energy (DOE) Office of Science, Office of Biological and Environmental Research, Atmospheric Systems Research (ASR) program. Pacific Northwest National Laboratory is operated for the DOE by Battelle Memorial Institute under contract no. DE-AC05-76RL01830. J.A.T. gratefully acknowledges support for FIGAERO HR-ToF-CIMS operation and analysis from DOE ASR grants DE-SC0006867 and DE-SC0011791. Funding for B.H.L. was provided by the NOAA Climate and Global Change Postdoctoral Fellowship. F.N.K. and

DOI: 10.1021/acs.est.6b01872
Environ. Sci. Technol. 2016, 50, 9872−9880

J.C.R. were supported by the National Science Foundation (AGS 1628491 and 1628530). J.D.S., Z.Z., and A.G. acknowledge support for organic synthesis of IEPOX from the National Science Foundation (NSF) grant CHE-1404644 and Environmental Protection Agency (EPA) grant R835404. Its contents are solely the responsibility of the grantee and do not necessarily represent the official views of EPA. Furthermore, the EPA does not endorse the purchase of any commercial products or services mentioned in the publication.

REFERENCES

(1) Guenther, A.; Karl, T.; Harley, P.; Wiedinmyer, C.; Palmer, P. I.; Geron, C. Estimates of global terrestrial isoprene emissions using MEGAN (Model of Emissions of Gases and Aerosols from Nature). *Atmos. Chem. Phys.* **2006**, *6*, 3181−3210.

(2) Henze, D. K.; Seinfeld, J. H. Global secondary organic aerosol from isoprene oxidation. *Geophys. Res. Lett.* **2006**, *33* (9), L09812.

(3) Hoyle, C. R.; Berntsen, T.; Myhre, G.; Isaksen, I. S. A. Secondary organic aerosol in the global aerosol − chemical transport model Oslo CTM2. *Atmos. Chem. Phys.* **2007**, *7* (21), 5675−5694.

(4) Claeys, M.; Graham, B.; Vas, G.; Wang, W.; Vermeylen, R.; Pashynska, V.; Cafmeyer, J.; Guyon, P.; Andreae, M. O.; Artaxo, P.; Maenhaut, W. Formation of secondary organic aerosols through photooxidation of isoprene. *Science* **2004**, *303* (5661), 1173−1176.

(5) Carlton, A. G.; Wiedinmyer, C.; Kroll, J. H. A review of Secondary Organic Aerosol (SOA) formation from isoprene. *Atmos. Chem. Phys.* **2009**, *9* (14), 4987−5005.

(6) Paulot, F.; Crounse, J. D.; Kjaergaard, H. G.; Kurten, A.; St Clair, J. M.; Seinfeld, J. H.; Wennberg, P. O. Unexpected Epoxide Formation in the Gas-Phase Photooxidation of Isoprene. *Science* **2009**, *325* (5941), 730−733.

(7) Lelieveld, J.; Butler, T. M.; Crowley, J. N.; Dillon, T. J.; Fischer, H.; Ganzeveld, L.; Harder, H.; Lawrence, M. G.; Martinez, M.; Taraborrelli, D.; Williams, J. Atmospheric oxidation capacity sustained by a tropical forest. *Nature* **2008**, *452* (7188), 737−740.

(8) Kiendler-Scharr, A.; Wildt, J.; Dal Maso, M.; Hohaus, T.; Kleist, E.; Mentel, T. F.; Tillmann, R.; Uerlings, R.; Schurr, U.; Wahner, A. New particle formation in forests inhibited by isoprene emissions. *Nature* **2009**, *461* (7262), 381−384.

(9) Jaoui, M.; Edney, E. O.; Kleindienst, T. E.; Lewandowski, M.; Offenberg, J. H.; Surratt, J. D.; Seinfeld, J. H. Formation of secondary organic aerosol from irradiated α-pinene/toluene/NOx mixtures and the effect of isoprene and sulfur dioxide. *J. Geophys. Res.* **2008**, *113*, D09303.

(10) Carslaw, K. S.; Lee, L. A.; Reddington, C. L.; Pringle, K. J.; Rap, A.; Forster, P. M.; Mann, G. W.; Spracklen, D. V.; Woodhouse, M. T.; Regayre, L. A.; Pierce, J. R. Large contribution of natural aerosols to uncertainty in indirect forcing. *Nature* **2013**, *503* (7474), 67−71.

(11) Crounse, J. D.; Paulot, F.; Kjaergaard, H. G.; Wennberg, P. O. Peroxy radical isomerization in the oxidation of isoprene. *Phys. Chem. Chem. Phys.* **2011**, *13* (30), 13607−13613.

(12) Lin, Y.-H.; Zhang, Z.; Docherty, K. S.; Zhang, H.; Budisulistiorini, S. H.; Rubitschun, C. L.; Shaw, S. L.; Knipping, E. M.; Edgerton, E. S.; Kleindienst, T. E.; Gold, A.; Surratt, J. D. Isoprene Epoxydiols as Precursors to Secondary Organic Aerosol Formation: Acid-Catalyzed Reactive Uptake Studies with Authentic Compounds. *Environ. Sci. Technol.* **2012**, *46* (1), 250−258.

(13) Paulot, F.; Henze, D. K.; Wennberg, P. O. Impact of the isoprene photochemical cascade on tropical ozone. *Atmos. Chem. Phys.* **2012**, *12* (3), 1307−1325.

(14) Crounse, J. D.; Nielsen, L. B.; Jørgensen, S.; Kjaergaard, H. G.; Wennberg, P. O. Autoxidation of Organic Compounds in the Atmosphere. *J. Phys. Chem. Lett.* **2013**, *4* (20), 3513−3520.

(15) Surratt, J. D.; Chan, A. W. H.; Eddingsaas, N. C.; Chan, M. N.; Loza, C. L.; Kwan, A. J.; Hersey, S. P.; Flagan, R. C.; Wennberg, P. O.; Seinfeld, J. H. Reactive intermediates revealed in secondary organic aerosol formation from isoprene. *Proc. Natl. Acad. Sci. U. S. A.* **2010**, *107* (15), 6640−6645.

(16) Lin, Y. H.; Zhang, H. F.; Pye, H. O. T.; Zhang, Z. F.; Marth, W. J.; Park, S.; Arashiro, M.; Cui, T. Q.; Budisulistiorini, H.; Sexton, K. G.; Vizuete, W.; Xie, Y.; Luecken, D. J.; Piletic, I. R.; Edney, E. O.; Bartolotti, L. J.; Gold, A.; Surratt, J. D. Epoxide as a precursor to secondary organic aerosol formation from isoprene photooxidation in the presence of nitrogen oxides. *Proc. Natl. Acad. Sci. U. S. A.* **2013**, *110* (17), 6718−6723.

(17) Lin, Y.-H.; Budisulistiorini, S. H.; Chu, K.; Siejack, R. A.; Zhang, H.; Riva, M.; Zhang, Z.; Gold, A.; Kautzman, K. E.; Surratt, J. D. Light-Absorbing Oligomer Formation in Secondary Organic Aerosol from Reactive Uptake of Isoprene Epoxydiols. *Environ. Sci. Technol.* **2014**, *48* (20), 12012−12021.

(18) Lin, Y. H.; Knipping, E. M.; Edgerton, E. S.; Shaw, S. L.; Surratt, J. D. Investigating the influences of SO_2 and NH_3 levels on isoprene-derived secondary organic aerosol formation using conditional sampling approaches. *Atmos. Chem. Phys.* **2013**, *13* (16), 8457−8470.

(19) Nguyen, T. B.; Coggon, M. M.; Bates, K. H.; Zhang, X.; Schwantes, R. H.; Schilling, K. A.; Loza, C. L.; Flagan, R. C.; Wennberg, P. O.; Seinfeld, J. H. Organic aerosol formation from the reactive uptake of isoprene epoxydiols (IEPOX) onto non-acidified inorganic seeds. *Atmos. Chem. Phys.* **2014**, *14* (7), 3497−3510.

(20) Zhang, X.; Cappa, C. D.; Jathar, S. H.; McVay, R. C.; Ensberg, J. J.; Kleeman, M. J.; Seinfeld, J. H. Influence of vapor wall loss in laboratory chambers on yields of secondary organic aerosol. *Proc. Natl. Acad. Sci. U. S. A.* **2014**, *111* (16), 5802−5807.

(21) Hallquist, M.; Wenger, J. C.; Baltensperger, U.; Rudich, Y.; Simpson, D.; Claeys, M.; Dommen, J.; Donahue, N. M.; George, C.; Goldstein, A. H.; Hamilton, J. F.; Herrmann, H.; Hoffmann, T.; Iinuma, Y.; Jang, M.; Jenkin, M. E.; Jimenez, J. L.; Kiendler-Scharr, A.; Maenhaut, W.; McFiggans, G.; Mentel, T. F.; Monod, A.; Prévôt, A. S. H.; Seinfeld, J. H.; Surratt, J. D.; Szmigielski, R.; Wildt, J. The formation, properties and impact of secondary organic aerosol: current and emerging issues. *Atmos. Chem. Phys.* **2009**, *9* (14), 5155−5236.

(22) Kroll, J. H.; Ng, N. L.; Murphy, S. M.; Flagan, R. C.; Seinfeld, J. H. Secondary organic aerosol formation from isoprene photooxidation under high-NOx conditions. *Geophys. Res. Lett.* **2005**, *32* (18), L18808.

(23) Liu, S.; Shilling, J. E.; Song, C.; Hiranuma, N.; Zaveri, R. A.; Russell, L. M. Hydrolysis of Organonitrate Functional Groups in Aerosol Particles. *Aerosol Sci. Technol.* **2012**, *46* (12), 1359−1369.

(24) Lindinger, W.; Hansel, A.; Jordan, A. On-line monitoring of volatile organic compounds at pptv levels by means of proton-transfer-reaction mass spectrometry (PTR-MS) medical applications, food control and environmental research. *Int. J. Mass Spectrom. Ion Processes* **1998**, *173* (3), 191−241.

(25) Lopez-Hilfiker, F. D.; Mohr, C.; Ehn, M.; Rubach, F.; Kleist, E.; Wildt, J.; Mentel, T. F.; Lutz, A.; Hallquist, M.; Worsnop, D.; Thornton, J. A. A novel method for online analysis of gas and particle composition: description and evaluation of a Filter Inlet for Gases and AEROsols (FIGAERO). *Atmos. Meas. Tech.* **2014**, *7* (4), 983−1001.

(26) Lee, B. H.; Lopez-Hilfiker, F. D.; Mohr, C.; Kurten, T.; Worsnop, D. R.; Thornton, J. A. An Iodide-Adduct High-Resolution Time-of-Flight Chemical-Ionization Mass Spectrometer: Application to Atmospheric Inorganic and Organic Compounds. *Environ. Sci. Technol.* **2014**, *48* (11), 6309−6317.

(27) DeCarlo, P. F.; Kimmel, J. R.; Trimborn, A.; Northway, M. J.; Jayne, J. T.; Aiken, A. C.; Gonin, M.; Fuhrer, K.; Horvath, T.; Docherty, K. S.; Worsnop, D. R.; Jimenez, J. L. Field-Deployable, High-Resolution, Time-of-Flight Aerosol Mass Spectrometer. *Anal. Chem.* **2006**, *78* (24), 8281−8289.

(28) Jayne, J. T.; Leard, D. C.; Zhang, X.; Davidovits, P.; Smith, K. A.; Kolb, C. E.; Worsnop, D. R. Development of an Aerosol Mass Spectrometer for Size and Composition Analysis of Submicron Particles. *Aerosol Sci. Technol.* **2000**, *33* (1−2), 49−70.

(29) Lopez-Hilfiker, F. D.; Iyer, S.; Mohr, C.; Lee, B. H.; D'Ambro, E. L.; Kurtén, T.; Thornton, J. A. Constraining the sensitivity of iodide adduct chemical ionization mass spectrometry to multifunctional organic molecules using the collision limit and thermodynamic stability of iodide ion adducts. *Atmos. Meas. Tech.* **2016**, *9* (4), 1505−1512.

DOI: 10.1021/acs.est.6b01872
Environ. Sci. Technol. 2016, 50, 9872−9880

(30) Lopez-Hilfiker, F. D.; Mohr, C.; Ehn, M.; Rubach, F.; Kleist, E.; Wildt, J.; Mentel, T. F.; Carrasquillo, A. J.; Daumit, K. E.; Hunter, J. F.; Kroll, J. H.; Worsnop, D. R.; Thornton, J. A. Phase partitioning and volatility of secondary organic aerosol components formed from alpha-pinene ozonolysis and OH oxidation: the importance of accretion products and other low volatility compounds. *Atmos. Chem. Phys.* **2015**, *15* (14), 7765−7776.

(31) Rivera-Rios, J. C.; Nguyen, T. B.; Crounse, J. D.; Jud, W.; St Clair, J. M.; Mikoviny, T.; Gilman, J. B.; Lerner, B. M.; Kaiser, J. B.; de Gouw, J.; Wisthaler, A.; Hansel, A.; Wennberg, P. O.; Seinfeld, J. H.; Keutsch, F. N. Conversion of hydroperoxides to carbonyls in field and laboratory instrumentation: Observational bias in diagnosing pristine versus anthropogenically controlled atmospheric chemistry. *Geophys. Res. Lett.* **2014**, *41* (23), 8645−8651.

(32) Wolfe, G. M.; Thornton, J. A. The Chemistry of Atmosphere-Forest Exchange (CAFE) Model - Part 1: Model description and characterization. *Atmos. Chem. Phys.* **2011**, *11* (1), 77−101.

(33) Jenkin, M. E.; Young, J. C.; Rickard, A. R. The MCM v3.3.1 degradation scheme for isoprene. *Atmos. Chem. Phys.* **2015**, *15* (20), 11433−11459.

(34) Butkovskaya, N. I.; Pouvesle, N.; Kukui, A.; Le Bras, G. Mechanism of the OH-initiated oxidation of glycolaldehyde over the temperature range 233−296 K. *J. Phys. Chem. A* **2006**, *110* (50), 13492−13499.

(35) Baeza-Romero, M. T.; Glowacki, D. R.; Blitz, M. A.; Heard, D. E.; Pilling, M. J.; Rickard, A. R.; Seakins, P. W. A combined experimental and theoretical study of the reaction between methylglyoxal and OH/OD radical: OH regeneration. *Phys. Chem. Chem. Phys.* **2007**, *9* (31), 4114−4128.

(36) Paulot, F.; Crounse, J. D.; Kjaergaard, H. G.; Kroll, J. H.; Seinfeld, J. H.; Wennberg, P. O. Isoprene photooxidation: new insights into the production of acids and organic nitrates. *Atmos. Chem. Phys.* **2009**, *9* (4), 1479−1501.

(37) Archibald, A. T.; Cooke, M. C.; Utembe, S. R.; Shallcross, D. E.; Derwent, R. G.; Jenkin, M. E. Impacts of mechanistic changes on HOx formation and recycling in the oxidation of isoprene. *Atmos. Chem. Phys.* **2010**, *10* (17), 8097−8118.

(38) Kroll, J. H.; Ng, N. L.; Murphy, S. M.; Flagan, R. C.; Seinfeld, J. H. Secondary organic aerosol formation from isoprene photooxidation. *Environ. Sci. Technol.* **2006**, *40* (6), 1869−1877.

(39) Wang, W.; Iinuma, Y.; Kahnt, A.; Ryabtsova, O.; Mutzel, A.; Vermeylen, R.; Van der Veken, P.; Maenhaut, W.; Herrmann, H.; Claeys, M. Formation of secondary organic aerosol marker compounds from the photooxidation of isoprene and isoprene-derived alkene diols under low-NOx conditions. *Faraday Discuss.* **2013**, *165*, 261−272.

(40) King, S. M.; Rosenoern, T.; Shilling, J. E.; Chen, Q.; Wang, Z.; Biskos, G.; McKinney, K. A.; Pöschl, U.; Martin, S. T. Cloud droplet activation of mixed organic-sulfate particles produced by the photooxidation of isoprene. *Atmos. Chem. Phys.* **2010**, *10* (8), 3953−3964.

(41) Surratt, J. D.; Murphy, S. M.; Kroll, J. H.; Ng, N. L.; Hildebrandt, L.; Sorooshian, A.; Szmigielski, R.; Vermeylen, R.; Maenhaut, W.; Claeys, M.; Flagan, R. C.; Seinfeld, J. H. Chemical Composition of Secondary Organic Aerosol Formed from the Photooxidation of Isoprene. *J. Phys. Chem. A* **2006**, *110* (31), 9665−9690.

(42) Riva, M.; Budisulistiorini, S. H. H.; Chen, Y.; Zhang, Z.; D'Ambro, E. L.; Zhang, X.; Gold, A.; Turpin, B. J.; Thornton, J. A.; Canagaratna, M. R.; Surratt, J. D. Chemical Characterization of Secondary Organic Aerosol from Oxidation of Isoprene Hydroxyhydroperoxides. *Environ. Sci. Technol.* **2016**, DOI: 10.1021/acs.est.6b02511.

(43) Krechmer, J. E.; Coggon, M. M.; Massoli, P.; Nguyen, T. B.; Crounse, J. D.; Hu, W.; Day, D. A.; Tyndall, G. S.; Henze, D. K.; Rivera-Rios, J. C.; Nowak, J. B.; Kimmel, J. R.; Mauldin, R. L.; Stark, H.; Jayne, J. T.; Sipilä, M.; Junninen, H.; St Clair, J. M.; Zhang, X.; Feiner, P. A.; Zhang, L.; Miller, D. O.; Brune, W. H.; Keutsch, F. N.; Wennberg, P. O.; Seinfeld, J. H.; Worsnop, D. R.; Jimenez, J. L.; Canagaratna, M. R. Formation of Low Volatility Organic Compounds and Secondary Organic Aerosol from Isoprene Hydroxyhydroperoxide Low-NO Oxidation. *Environ. Sci. Technol.* **2015**, *49* (17), 10330−10339.

(44) Jokinen, T.; Berndt, T.; Makkonen, R.; Kerminen, V.-M.; Junninen, H.; Paasonen, P.; Stratmann, F.; Herrmann, H.; Guenther, A. B.; Worsnop, D. R.; Kulmala, M.; Ehn, M.; Sipilä, M. Production of extremely low volatile organic compounds from biogenic emissions: Measured yields and atmospheric implications. *Proc. Natl. Acad. Sci. U. S. A.* **2015**, *112* (23), 7123−7128.

(45) Bates, K. H.; Crounse, J. D.; St Clair, J. M.; Bennett, N. B.; Nguyen, T. B.; Seinfeld, J. H.; Stoltz, B. M.; Wennberg, P. O. Gas Phase Production and Loss of Isoprene Epoxydiols. *J. Phys. Chem. A* **2014**, *118* (7), 1237−1246.

(46) Chen, Q.; Liu, Y.; Donahue, N. M.; Shilling, J. E.; Martin, S. T. Particle-Phase Chemistry of Secondary Organic Material: Modeled Compared to Measured O:C and H:C Elemental Ratios Provide Constraints. *Environ. Sci. Technol.* **2011**, *45* (11), 4763−4770.

(47) Lee, B. H.; Mohr, C.; Lopez-Hilfiker, F. D.; Lutz, A.; Hallquist, M.; Lee, L.; Romer, P.; Cohen, R. C.; Iyer, S.; Kurtén, T.; Hu, W.; Day, D. A.; Campuzano-Jost, P.; Jimenez, J. L.; Xu, L.; Ng, N. L.; Guo, H.; Weber, R. J.; Wild, R. J.; Brown, S. S.; Koss, A.; de Gouw, J.; Olson, K.; Goldstein, A. H.; Seco, R.; Kim, S.; McAvey, K.; Shepson, P. B.; Starn, T.; Baumann, K.; Edgerton, E. S.; Liu, J.; Shilling, J. E.; Miller, D. O.; Brune, W.; Schobesberger, S.; D'Ambro, E. L.; Thornton, J. A. Highly functionalized organic nitrates in the southeast United States: Contribution to secondary organic aerosol and reactive nitrogen budgets. *Proc. Natl. Acad. Sci. U. S. A.* **2016**, *113* (6), 1516−1521.

(48) Xu, L.; Kollman, M. S.; Song, C.; Shilling, J. E.; Ng, N. L. Effects of NOx on the Volatility of Secondary Organic Aerosol from Isoprene Photooxidation. *Environ. Sci. Technol.* **2014**, *48* (4), 2253−2262.

(49) Gaston, C. J.; Riedel, T. P.; Zhang, Z.; Gold, A.; Surratt, J. D.; Thornton, J. A. Reactive Uptake of an Isoprene-Derived Epoxydiol to Submicron Aerosol Particles. *Environ. Sci. Technol.* **2014**, *48* (19), 11178−11186.

(50) Matsunaga, A.; Ziemann, P. J. Gas-Wall Partitioning of Organic Compounds in a Teflon Film Chamber and Potential Effects on Reaction Product and Aerosol Yield Measurements. *Aerosol Sci. Technol.* **2010**, *44* (10), 881−892.

(51) Ehn, M.; Thornton, J. A.; Kleist, E.; Sipila, M.; Junninen, H.; Pullinen, I.; Springer, M.; Rubach, F.; Tillmann, R.; Lee, B.; Lopez-Hilfiker, F.; Andres, S.; Acir, I.-H.; Rissanen, M.; Jokinen, T.; Schobesberger, S.; Kangasluoma, J.; Kontkanen, J.; Nieminen, T.; Kurten, T.; Nielsen, L. B.; Jorgensen, S.; Kjaergaard, H. G.; Canagaratna, M.; Maso, M. D.; Berndt, T.; Petaja, T.; Wahner, A.; Kerminen, V.-M.; Kulmala, M.; Worsnop, D. R.; Wildt, J.; Mentel, T. F. A large source of low-volatility secondary organic aerosol. *Nature* **2014**, *506* (7489), 476−479.

(52) Shilling, J. E.; Chen, Q.; King, S. M.; Rosenoern, T.; Kroll, J. H.; Worsnop, D. R.; McKinney, K. A.; Martin, S. T. Particle mass yield in secondary organic aerosol formed by the dark ozonolysis of alpha-pinene. *Atmos. Chem. Phys.* **2008**, *8* (7), 2073−2088.

(53) Dommen, J.; Metzger, A.; Duplissy, J.; Kalberer, M.; Alfarra, M. R.; Gascho, A.; Weingartner, E.; Prevot, A. S. H.; Verheggen, B.; Baltensperger, U. Laboratory observation of oligomers in the aerosol from isoprene/NOx photooxidation. *Geophys. Res. Lett.* **2006**, *33* (13), L13805.

(54) Zhang, H.; Surratt, J. D.; Lin, Y. H.; Bapat, J.; Kamens, R. M. Effect of relative humidity on SOA formation from isoprene/NO photooxidation: enhancement of 2-methylglyceric acid and its corresponding oligoesters under dry conditions. *Atmos. Chem. Phys.* **2011**, *11* (13), 6411−6424.

DOI: 10.1021/acs.est.6b01872
Environ. Sci. Technol. 2016, 50, 9872−9880